

AD-A110 565

NAVAL RESEARCH LAB WASHINGTON DC

F/8 20/7

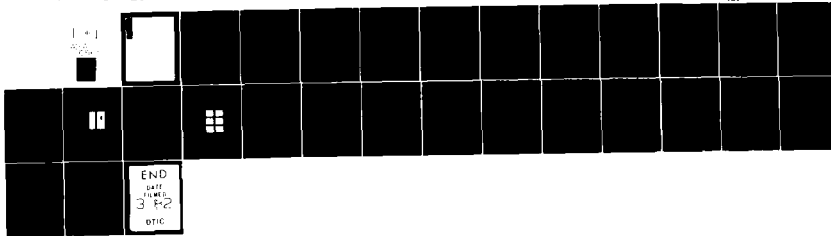
REPETITIVE OPERATION OF AN INDUCTIVELY DRIVEN ELECTRON-BEAM DIO--ETC(U)

JAN 82 B FELL, R J COMMISSO, V E SCHERRER

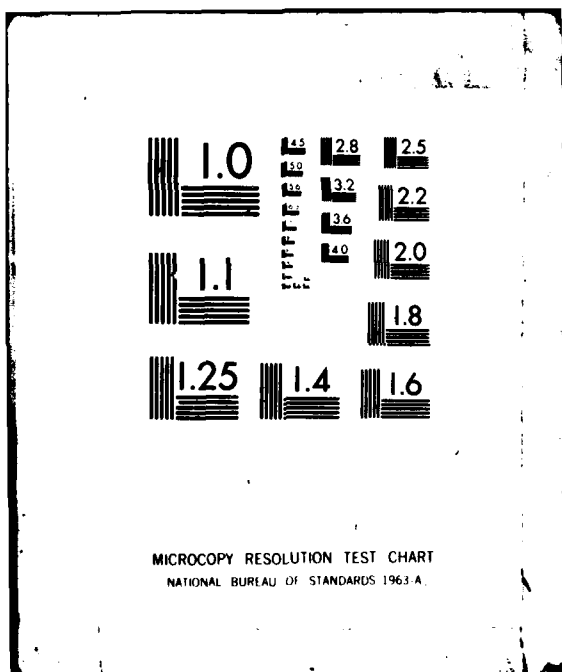
UNCLASSIFIED

NRL-MR-4714

NI



END
100-
3 F 2
DTIC



AD A110565

SECURITY CLASSIFICATION OF THIS PAGE (When Data Entered)

REPORT DOCUMENTATION PAGE		READ INSTRUCTIONS BEFORE COMPLETING FORM
1. REPORT NUMBER	2. GOVT ACCESSION NO.	3. RECIPIENT'S CATALOG NUMBER
NRL Memorandum Report 4714		AD-A110 565
4. TITLE (and Subtitle)	5. TYPE OF REPORT & PERIOD COVERED	
REPETITIVE OPERATION OF AN INDUCTIVELY DRIVEN ELECTRON-BEAM DIODE		Interim report on a continuing NRL problem
6. PERFORMING ORG. REPORT NUMBER		
7. AUTHOR(s)	8. CONTRACT OR GRANT NUMBER(s)	
B. Fell ^{a,b} , R. J. Commissio ^a , V. E. Scherrer, and I. M. Vitkovitsky		
9. PERFORMING ORGANIZATION NAME AND ADDRESS	10. PROGRAM ELEMENT, PROJECT, TASK AREA & WORK UNIT NUMBERS	
Naval Research Laboratory Washington, DC 20375	61153N, RR0110941 47-0878-0-2	
11. CONTROLLING OFFICE NAME AND ADDRESS	12. REPORT DATE	
Naval Research Laboratory Washington, DC 20375	January 11, 1982	
13. NUMBER OF PAGES	28	
14. MONITORING AGENCY NAME & ADDRESS (if different from Controlling Office)	15. SECURITY CLASS. (of this report)	
	UNCLASSIFIED	
	15a. DECLASSIFICATION/DOWNGRADING SCHEDULE	
16. DISTRIBUTION STATEMENT (of this Report)		
Approved for public release; distribution unlimited.		
17. DISTRIBUTION STATEMENT (of the abstract entered in Block 2u, if different from Report)	S FEB 4 1982	
18. SUPPLEMENTARY NOTES		
^a Jaycor, Inc., 205 S. Whiting Street, Alexandria, VA 22302 ^b Institut Fuer Hochspannungs Technik, Braunschweig, Federal Republic of Germany		
19. KEY WORDS (Continue on reverse side if necessary and identify by block number)		
Electron beam diode recovery Inductive storage pulsers		
20. ABSTRACT (Continue on reverse side if necessary and identify by block number)	<i>Recovery of pulsed electron beam diodes operating in the 50 A/cm² range has been studied using an inductive storage source producing two 100-200 kV pulses with separation ranging from 10-500 μs. The diode cannot instantaneously support a second voltage pulse because of the effective short circuit provided by the interelectrode plasma associated with the first pulse. After a period of 100 μs, the voltage applied to the diode is not short-circuited and a second electron beam, nearly identical to the first, is formed.</i>	

DD FORM 1 JAN 73 1473 EDITION OF 1 NOV 68 IS OBSOLETE
S/N 0102-014-6601

SECURITY CLASSIFICATION OF THIS PAGE (When Data Entered)

TABLE OF CONTENTS

I.	INTRODUCTION.....	1
II.	EXPERIMENTAL CONFIGURATION.....	2
	A. Pulser Circuit.....	2
	B. Diode Geometry.....	5
	C. Diagnostics.....	5
III.	SINGLE PULSE OPERATION.....	6
	A. Beam Generation and Characteristics.....	6
	B. Plasma Formation and Life Time.....	8
	C. Diode Conditioning Effect.....	10
IV.	DOUBLE PULSE OPERATION.....	12
V.	DISCUSSION.....	15
VI.	CONCLUSION.....	18
	ACKNOWLEDGEMENTS.....	18
	REFERENCES.....	21



Accession For
CRA&I
IC T48
Approved
Classification

DTIC
Distribution/
Availability
Avail. Gr.
Special

Dist	

REPETITIVE OPERATION OF AN INDUCTIVELY DRIVEN ELECTRON-BEAM DIODE

I. INTRODUCTION

Repetitive pulsed operation of electron-beam producing diodes is presently needed for certain switching experiments¹ and may have future application to flash x-radiography, laser technology² or inertial confinement fusion. The latter two applications require very large energies as well. Consequently, an economical approach may require the pulse generator to be based on inductive energy storage. Such pulse generators have already been used to produce electron beams^{3,4} with currents of a few kiloamperes and accelerating voltages of 1.5 to 2.0 MV. Moreover, substantially higher power levels are now attainable from inductive storage systems.^{5,6} As a consequence, the time is now appropriate to investigate multiple pulse operation of electron beam diodes from an inductive storage system, made possible by the recent advent of cascade switching.⁷

Diodes have been operated repetitively at a rate of 30 Hz⁸ but studies of multiple pulses separated by an interval of the order of 100 μ sec are unknown. The limitation on the time interval between pulses due to diode recovery has not heretofore received attention. At high current density, diode space-charge limited impedance is affected by the appearance of plasma.⁹ Some control by an external magnetic field has been used to suppress partly plasma effects, e.g., as done in foiless diodes.^{10,11} Such plasma formation during and after beam generation may affect the diode characteristic for subsequent pulses in repetitive systems. These effects are particularly important in inductive systems because of their characteristically long L/R decay time and slow (compared to capacitive systems) risetime. The plasma production in the diode and its recovery characteristics are also related to the processes occurring in vacuum current interrupters, including those being developed for repetitive switching.¹²

Experiments to study production of repetitively pulsed electron beams from an inductive store are reported here. A circuit that uses a two-stage opening switch module¹³ produces an electron beam with \sim 150 keV particle energy, \lesssim 1 kA current and \sim 0.5 μ sec pulse duration. By straightforward modification, this circuit was used for two pulse operation with a variable

interpulse separation of 10-500 μ sec. Plasma formation and life-time and their effects on the performance of a doubly pulsed diode have also been studied, typically at beam current densities of ~ 50 A/cm².

II. EXPERIMENTAL CONFIGURATION

A. Pulser Circuit

A schematic of the circuit is shown in Fig. 1. Basically, a capacitor current source is used to charge an inductive store with exploding wire fuses (in air) serving as the opening switches that provide either one or two high voltage pulses across an electron beam diode. As is well known, the peak voltage across a fuse wire depends upon the wire length, its cross section, the vaporization velocity, the material from which it is made and the medium surrounding the wire.¹³⁻¹⁶ To obtain the maximum peak induced voltage one needs very rapid explosions of long, thin wires by fast rising current pulses. High voltage (relative to the capacitor charging voltage of < 10 kV) pulses across the diode were produced by sequencing two wire fuses for each pulse. This staging enhances the high voltage production because the rapid rise of the current in the second stage allows for a thinner fuse wire and therefore a shorter time to completion of vaporization.

The first voltage pulse to appear across the diode, shown in Fig. 2, is generated by staging of fuse F_1 and F_2 (Fig 1). These fuses are also used for single pulse operation, which is achieved by removing fuses F_3 , F_4 and F_{D2} from the system. The first pulse is generated by triggering spark gap S_1 at time t_0 (Fig. 2) thus charging of the inductance L through F_1 . The first stage fuse, F_1 , works as an opening switch that is not optimized to high voltage production but rather serves to commutate, with relatively small losses, a high current pulse i_1 , into the next stage via the self-breakdown of spark gap, S_2 , at time t_1 . The smaller diameter fuse F_2 , in response to

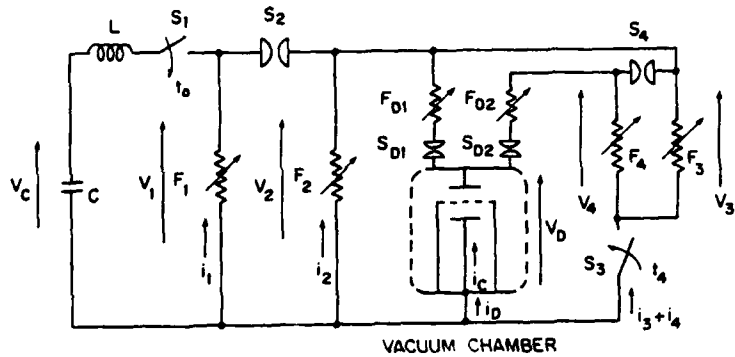


Fig. 1. Circuit diagram of the system with two pulse cascade switching.

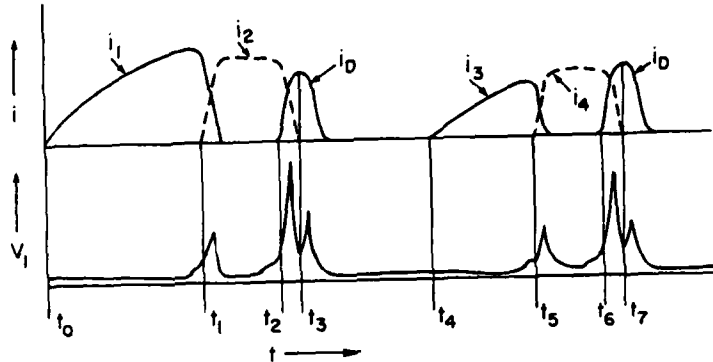


Fig. 2. Current and voltage waveforms with arbitrary amplitude and time scales depicting two-pulse operation.

current i_2 , generates a high voltage pulse across the diode after self-breakdown of sharpening gap S_{D1} at time t_2 . Fuse F_{D1} operates as a fast opening switch starting at time t_3 , interrupting the diode discharge current. The diode current flow duration is controlled by the cross section of this fuse (Table I).

Table I: Dependence of current flow duration on diode fuse (F_{D1} and F_{D2}) cross sections

Fuse Type	Cross-Section (mm^2)	Time (μsec)
1	0.0016	1-2
2	0.0081	2-3
3	0.018	7
4	0.051	11
5	0.013	6

To generate a second high voltage pulse across the diode another two stage network (fuses F_3 , F_4 and F_{D2}), similar to the first one, is added to the system and switched into the circuit at time t_4 by an explosively driven closing switch,¹⁷ S_3 . This switch holds off the entire voltage associated with the first pulse, closes within few microseconds into a high conducting state, and, by external triggering, can control the interpulse separation times to be between 10 μ sec and 500 μ sec.

The size of wires is determined not only by voltage generation requirements, but also by the necessity to hold off the voltage produced by all fuses exploding later. As the dielectric strength of an exploded wire decreases with time after explosion,¹³ the wires of the first pulse forming network (during double pulse operation) have to be much longer than necessary for optimal peak voltage production. This causes lower first pulse peak voltages with double pulse operation than with single pulse operation (120 kV instead of 180 kV). Table II shows a summary of wire and switch parameters used. All spark gaps were at atmospheric pressure and set for self-breakdown, except S_1 which was command triggered.

Table II: Typical Circuit Data

Capacitive store : $C = 240 \mu F$, $V_0 = 9 \text{ kV}$
 Inductive store: $L = 7 \mu H$

a) Single Pulse Operation:

<u>Fuse (Fig. 1)</u>	F_1	F_2	F_{D1}
Length (cm)	23	20	20
Cross Section (mm^2)	0.1	0.013	0.0016-0.05
Peak current (kA)	21	11	--
<u>Spark gap (Fig. 1)</u>		S_2	S_{D1}
Spark gap spacing (mm)		10	13

b) Double Pulse Operation

<u>Fuse (Fig 1)</u>	F_1	F_2	F_{D1}	F_3	F_4	F_{D2}
Length (cm)	37	33	20	21	22	20
Cross-section (mm^2)	0.15	0.04	0.0016	0.1	0.026	0.0016
Peak current (kA)	30	13	--	10	7	--
<u>Spark gap (Fig. 1)</u>		S_2	S_{D1}		S_4	S_{D2}
Spark gap spacing (mm)		8	10		10	13

B. Diode Geometry

The basic diode geometry is illustrated in Figure 3. The diode used in these studies has a copper screen anode with an optional 7.5 μm thick aluminum foil to allow only the high energy portion of the electron beam to reach a collector plate located behind the anode-cathode gap and to prevent plasma from reaching the collector. For these experiments the cathode consisted of sawblades or carbon felt. Unless otherwise stated, the results shown will be for the sawblade cathodes. The anode shield, used for defining the beam cross section incident on the collector, was 10 cm in diameter.

C. Diagnostics

Diagnostics consisted of a voltage divider to measure the diode voltage, V_D ; calibrated Rogowski loops to measure the diode current, i_D , and collector current, i_C (Fig. 1); a streak camera to observe the light emitted by the diode plasma; and a photomultiplier with collimation optics to provide spatial resolution along a line of sight perpendicular to the axis of the diode. The time-integrated beam spatial characteristics were obtained using a thin film dosimeter.

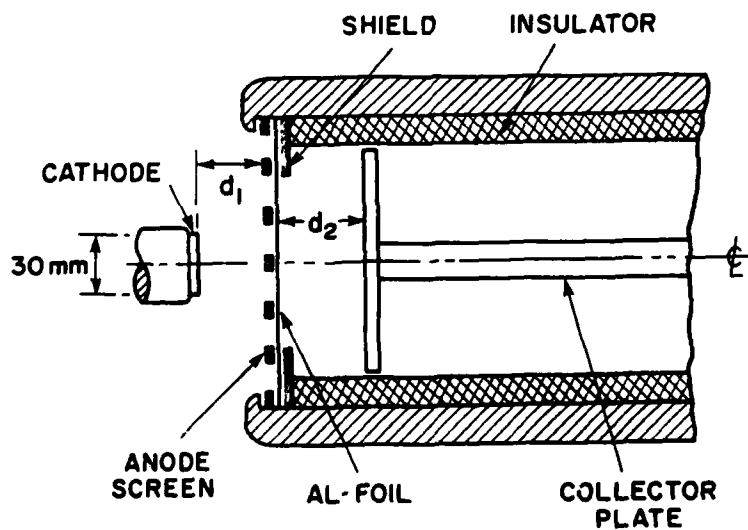


Fig. 3. Schematic of the electrodes and collector structure of the diode.

III. SINGLE PULSE OPERATION

A. Beam Generation and Characteristics

The current and voltage across the diode for a cathode area of 7 cm^2 and an anode-cathode gap of 1.5 cm as well as the electron beam current into collector and the diode impedance are shown in Fig. 4. The inductive component of the diode voltage was < 5% of the signal and was therefore neglected. The voltage pulse risetime, consisting of two different components, is determined by the characteristics of the switch (S_2) closing and fuse (F_2) opening. The diode current of about 1 kA, consists initially of the electron beam (part of which is also intercepted by the collector) and in later phases ($> 250 \text{ nsec}$) of the plasma current. This late time current is not directly associated with the beam (as evidenced by i_c decreasing after $\sim 250 \text{ nsec}$) but rather is being carried by the low voltage arc plasma¹⁸ that forms in the anode-cathode gap subsequent to the beam generation. The behavior of the diode impedance, Z , in the pre-arc phase is typical for diodes where plasma, formed at electron emission sites (whiskers) and possibly at the anode, expands into a region between the electrodes. The impedance collapse at times $\gtrsim 250 \text{ nsec}$ is a result of this whisker plasma providing a short circuit across the diode. The diode plasma moves across the gap at an average speed of $3-5 \times 10^6 \text{ cm/sec}$ as determined by the anode-cathode separation and the time, t_p (Fig. 4), at which time the diode current is being carried primarily by the arc plasma in the diode. The time of onset and rate of collapse are consistent with the parameters reported elsewhere.^{9,19}

The time averaged relative density distribution of the beam at the anode was estimated using a thin film dosimeter, commonly known as blue cellophane.²⁰ The $25 \mu\text{m}$ thick cellophane was placed directly behind the anode foil (Fig. 3). After exposure to the electron beam, the cellophane was scanned to obtain a white light transmission characteristic, an example of which is shown in Fig. 5. To obtain the curves in Fig. 5, points of maximum exposure were located by visual inspection and orthogonal, scans made through them. The radial scale is referenced to the geometrical axis of the diode ($r=0$) and the profiles represent a superposition of seven shots. The data suggest that the beam has a somewhat hollow profile, is non-circular, and is centered off the diode axis. Field enhancement at the diode edge may be responsible for the hollow beam profile and the displacement of diode axis

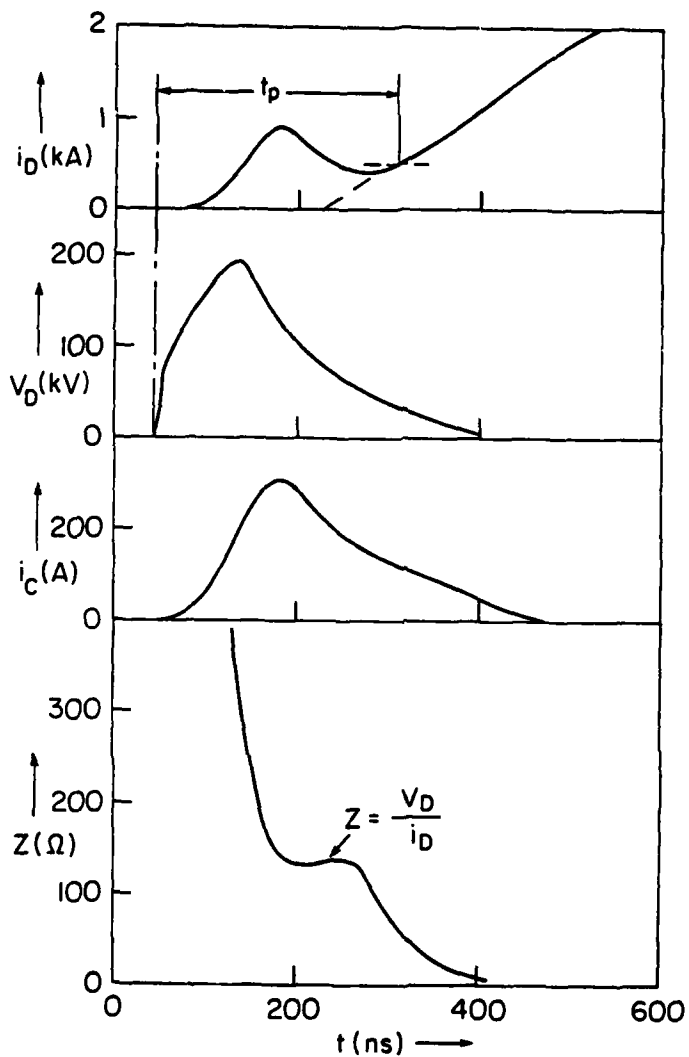


Fig. 4 Current i_D and voltage V_D across the electron beam diode. Also shown are the component of the electron beam measured by the collector plate, i_c and diode impedance determined from i_D and V_D .

from beam axis may result from a misalignment of either the cathode, or anode, or both. By taking a sequence of varying exposures on different pieces of cellophane the beam reproducibility and linearity of the technique can be checked. Results of accumulating doses for 1, 4, 6 and 7 shots are shown in Fig. 6. The general features of the curves are reproduced in each case indicating that the beam's spatial distribution is fairly reproducible on the average. From these and similar data the change in white light transmission

at a single radius as a function of shot number can be obtained and is plotted in Fig. 7. The data indicates a nearly linear response of the cellophane to dosage. Using this method, the beam area at the anode was determined to be $\sim 20 \text{ cm}^2$ giving a mean beam current density at the anode of 50 A/cm^2 .

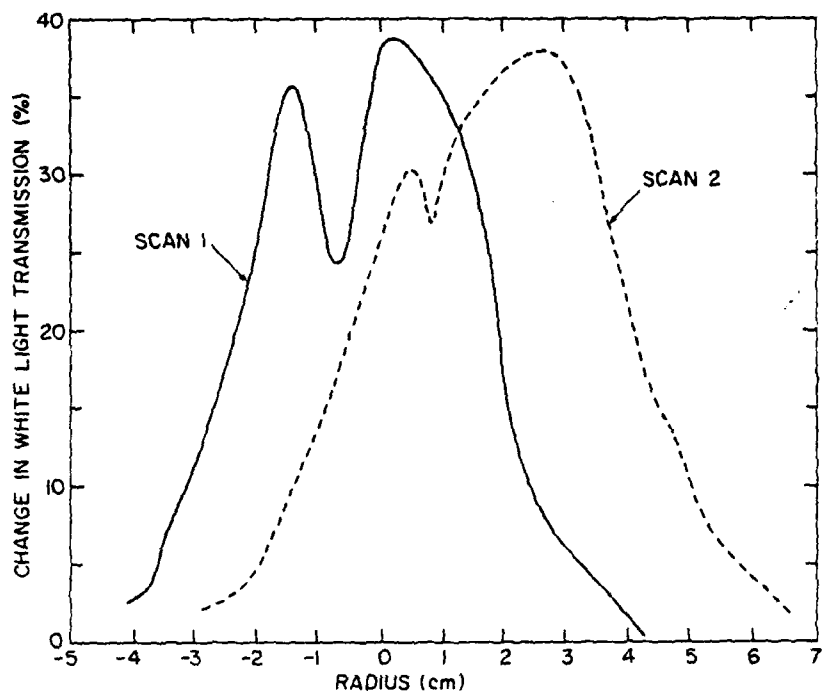


Fig. 5 White light transmission characteristics for blue cellophane. Scans were taken horizontally (Scan 1) and vertically (Scan 2) exposures.

B. Plasma Formation and Life Time

The plasma in the diode, present after the impedance collapse, has been observed with a streak camera and collimated photomultiplier. The streak camera, with a slit aligned perpendicular to the diode axis (Fig. 8) shows the appearance of plasma (with sufficient density to expose the film) at about 500 nsec after voltage application to the diode. This is a little later than the onset of the diode current associated with plasma, as seen in Fig. 8, and later than the time, t_p , shown in Fig. 4. The light emission recorded by the streak camera suggests that the light associated with the whisker plasma is of insufficient intensity to be recorded on the film. It follows from this that

the arc plasma dominates the plasma production when an inductive storage system with post-pulse current is used. To reduce the effects of this current a fuse F_{D1} (shown in the diagram of Fig. 1) is used. The choice of cross section for this fuse determines the time when the diode current can be interrupted. The earlier the interruption, the less plasma is produced.

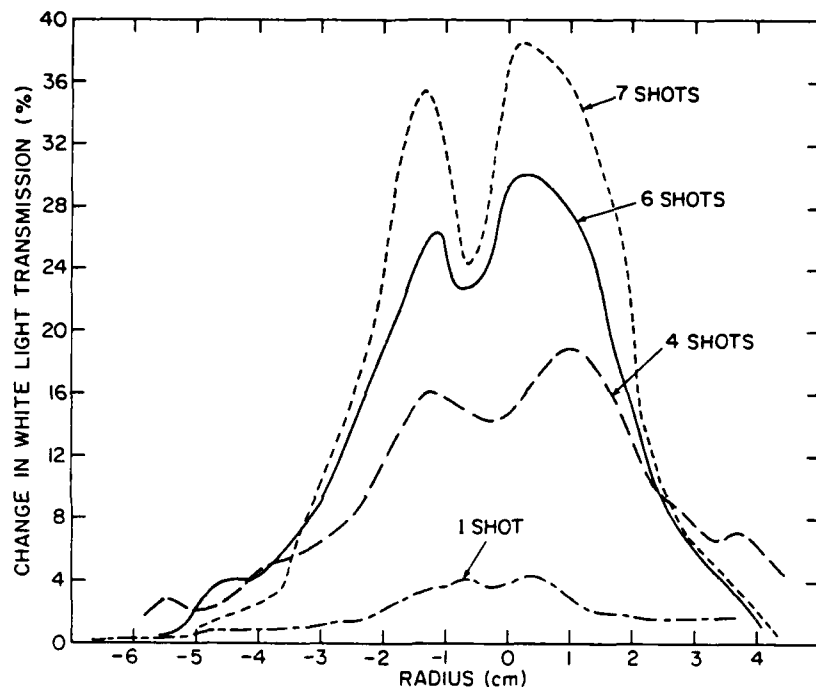


Fig. 6 White light transmission characteristic for blue cellophane with 1, 4, 6 and 7 exposures.

A typical time history of the light emission as observed by the photomultiplier and the photomultiplier viewing geometry are illustrated in Fig. 9. As can be seen from the figure, the peak light emission amplitude increases and decreases with the peak plasma current in the diode. The light, however, persists for some microseconds after the current has ceased. The persistence may be a consequence of the characteristic recombination and plasma expansion times. This point will be discussed further.

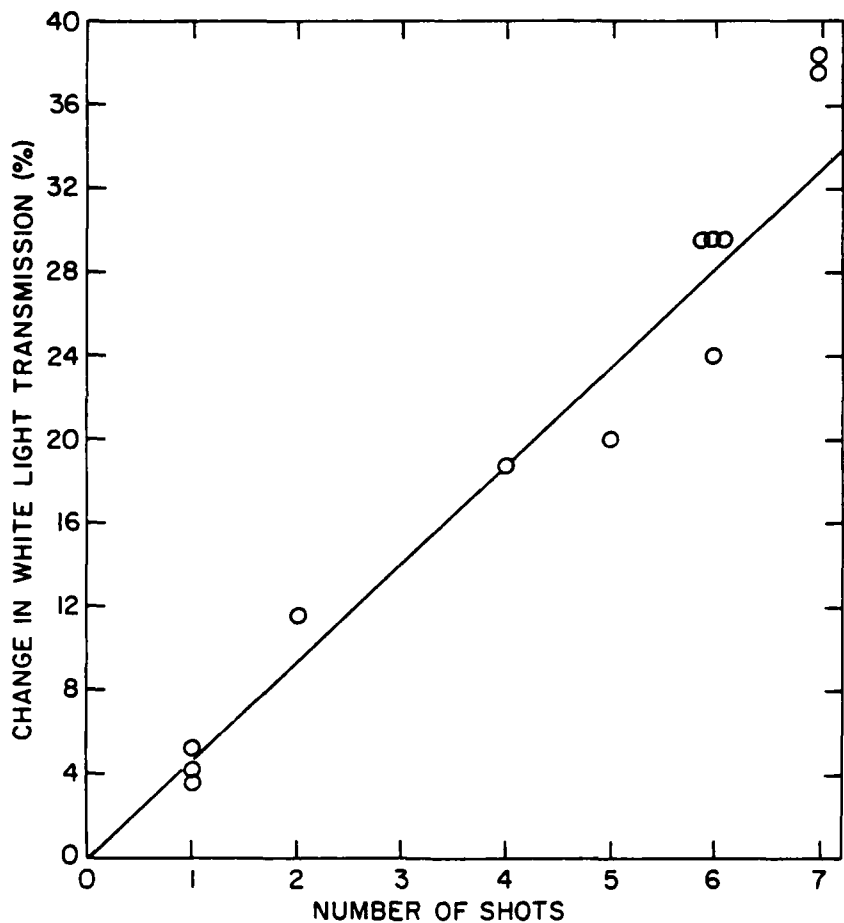


Fig. 7. White light transmission as a function of exposure for blue cellophane.

C. Diode Conditioning Effect

A conditioning effect was observed for single-pulse operation and is illustrated in Fig. 10. This effect appears to be correlated with the duration of arc plasma current which flowed in the diode in the previous shot. In the figure, collector current (proportional to the beam current) and diode voltage waveforms for six consecutive single-pulse shots are reproduced. As can be seen, the beam current in the second shot is reduced or enhanced depending on whether the plasma current of the preceding shot is small or large, respectively, as indicated by the current waveforms at the

bottom of the figure. The plasma current duration is controlled by the choice of fuse 1 or 2 (Table 1 and Fig. 10). The arc plasma consequently has a conditioning effect on the cathode. Possibly the cathode whiskers are enhanced on the higher arc current shots, or the hydrocarbons coating the cathode may crack owing to additional heating associated with the higher current leaving an increased concentration of carbon.

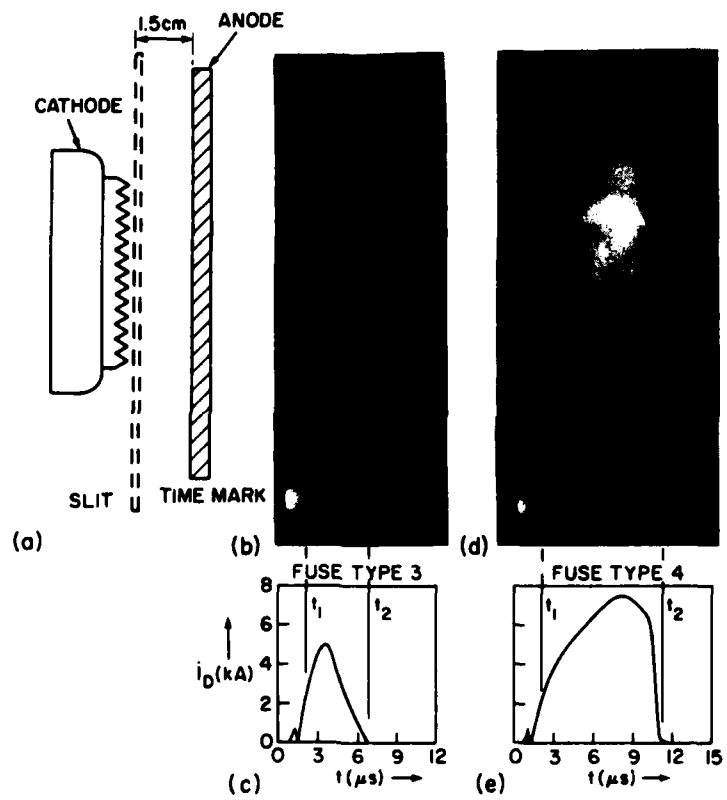


Fig. 8 Time correlation between diode current, i_D , for fuses (3 and 4 shown in Table 1) and plasma luminosity as measured by a streak camera. Sketch at left indicates the area observed by the viewing slit.

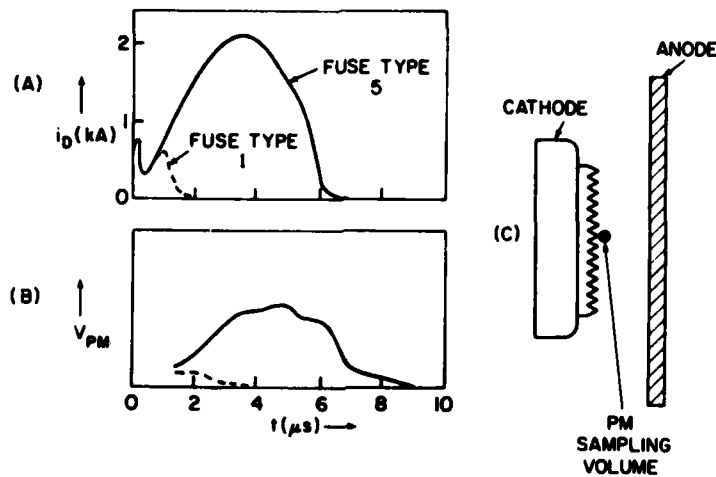


Fig. 9. Diode current (A) and photomultiplier signal (B) for fuse diameters of 50 μ m (dashed curves) and 140 μ m (solid curves). Also shown is the photomultiplier viewing geometry (C).

IV. DOUBLE PULSE OPERATION

The diode characteristics for the second pulse are shown in Fig. 11 (in analogy to Fig. 4 for single pulse operation). Type 1 discharges, indicated by solid lines, show a similar behavior to the single pulse. The delay between pulses necessary to obtain the behavior is $\gtrsim 100 \mu$ sec. Not clear in Fig. 11 but evident in the actual data is the observation that the second electron beam is emitted earlier relative to the second voltage pulse when compared to the relative time histories of the beam current and voltage of the first pulse (i.e., of the fully recovered diode). This most likely is a result of the change in diode environment brought about by the first pulse. The early time behavior of the second voltage pulse also differs from that of the first. This may be caused by the diode environment or the details of the second pulse circuitry. In general the beam current and voltage are lower for the second pulse than for the first owing primarily to the fact that much of the stored energy is consumed in producing the first pulse.

Type 2 discharges, indicated by the dashed lines in Fig. 11, result when the delay between pulses is $\lesssim 100 \mu$ sec and are not always reproducible. That is, infrequently type 1 discharges occur at the shorter inter-pulse delay. It

can be noted that even though the gap appears to be shorted for type 2 discharges a low current beam may still be produced ($i_c \neq 0$ for type 2 discharges in Fig. 11).

The diode impedance at maximum voltage (V_{max}/i_D) for various inter-pulse separation times, Δt , is plotted in Fig. 12 for both sawblade (open characters) and carbon felt cathodes (solid characters). In both cases the triangles are data obtained for type 2 discharges and the circles are associated with type 1 discharges (Fig. 11). The diode impedance for the second pulse with the

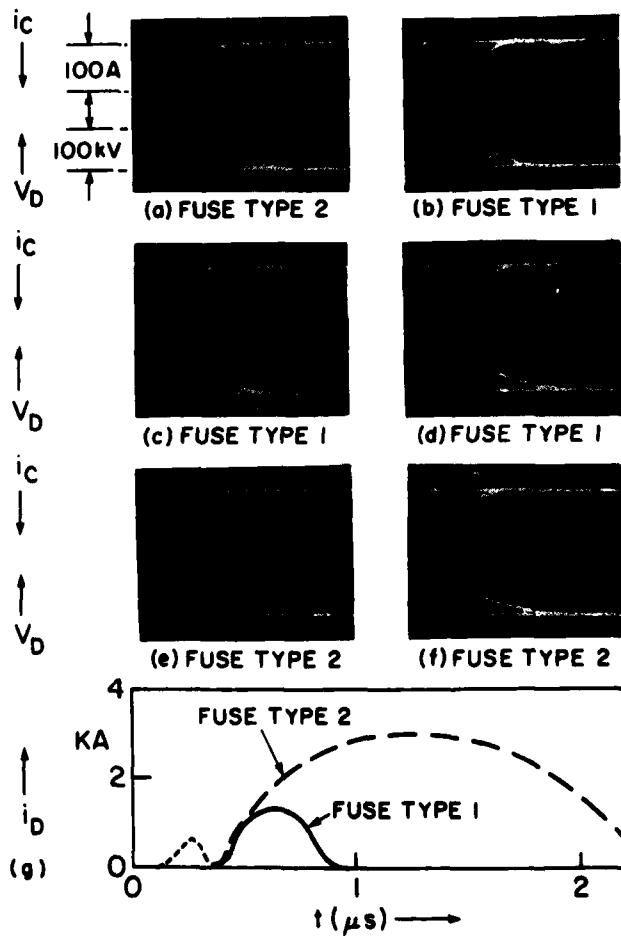


Fig. 10 Sequence of shots illustrating conditioning effects on subsequent shots.

sawblade cathode for $\Delta t \gtrsim 100 \mu\text{sec}$ is $\sim 250 \Omega$ and with carbon felt for $\Delta t \gtrsim 200 \mu\text{sec}$ is $\sim 75 \Omega$. Both of these values, as indicated on the figure, agree with the impedance observed for the first pulse, i.e., fully recovered diode. Note, however, that even though the impedance is the same for the two pulses, the detailed beam current and voltage waveforms are not identical in all cases as discussed in the preceding paragraph.

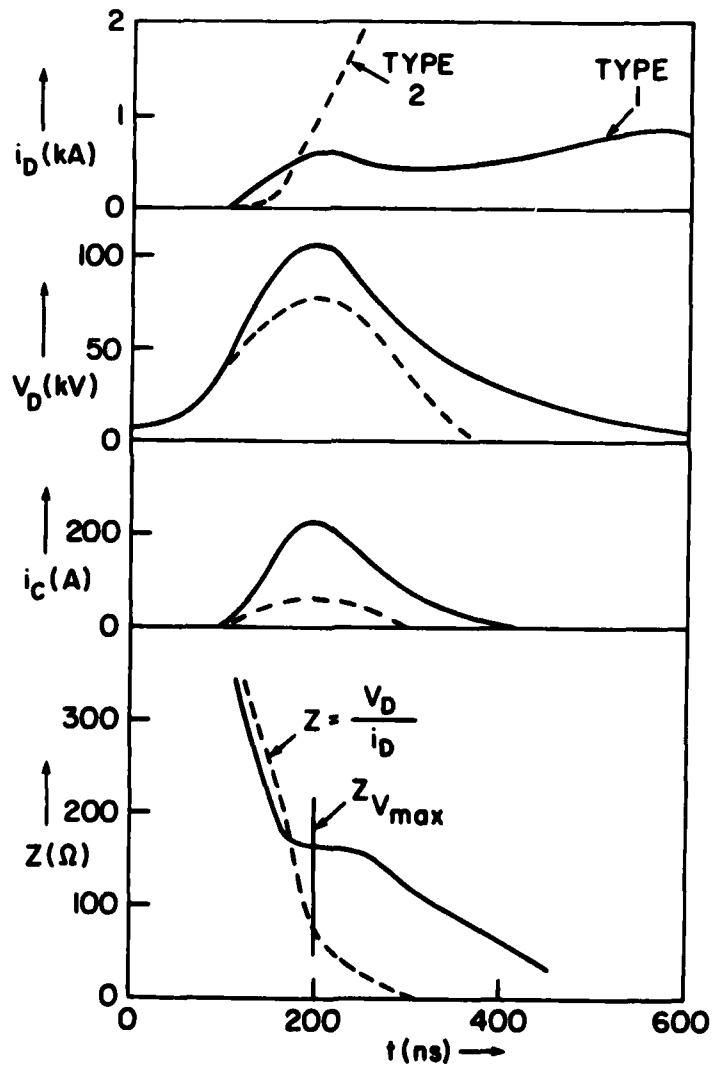


Fig. 11. Current, i_D and voltage V_D , for the second pulse across the diode. Also shown are the collector currents, i_c , and diode impedances, Z .

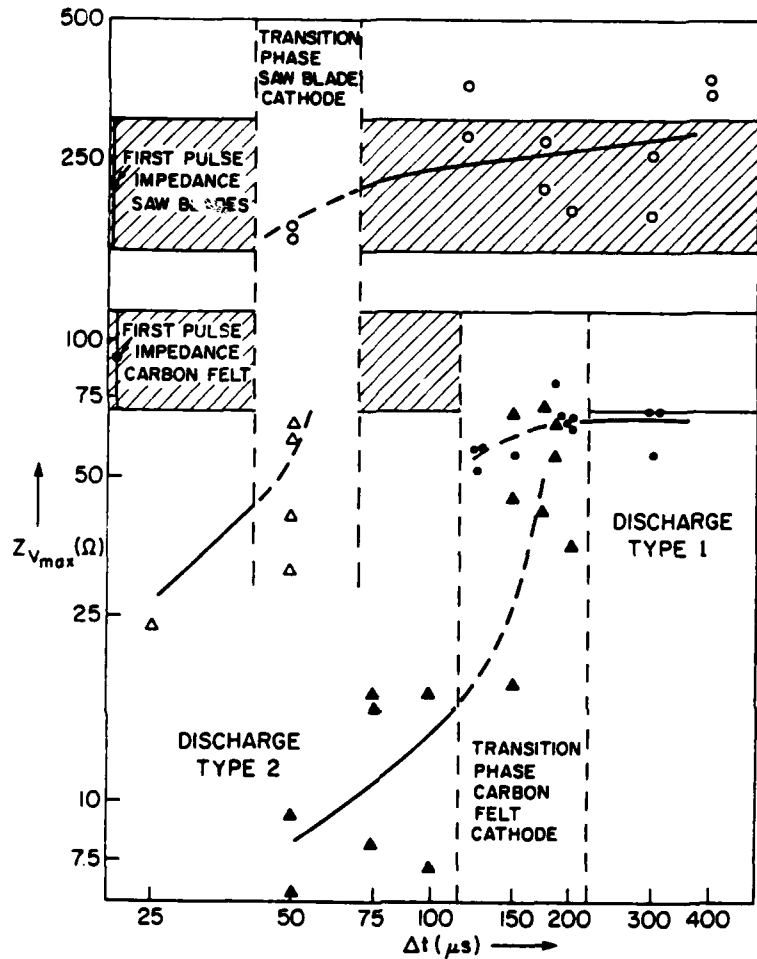


Fig. 12. Second pulse diode impedance (at the time of peak voltage) shown as function of the pulse separation time, for sawblade (open characters) and carbon felt (solid characters) cathodes. Triangles indicate type 2 discharges and circles indicate type 1 discharges.

V. DISCUSSION

Plasma formation in electron beam diodes using field emission cathodes has been extensively studied. Parker⁹ provides a review of plasma formation mechanisms and their effects on the impedance of high current diodes. The mechanisms outlined here are based on this review. The initial diode plasma is associated with explosion of whiskers on the cathode surface and follows stable field emission. These whiskers can carry current densities ranging

from 10^6 to 10^8 A/cm 2 , which cause strong local heating. The electric field, F_w , at the whisker tip is enhanced on the order of 100 times relative to the average applied field across the anode-cathode gap causing emission of electrons. The electron current is determined by the Child-Langmuir space charge limitation which is modified by the expanding cathode whisker plasma. The effect of the plasma on the diode impedance is determined from both the time of onset of plasma formation, $t_0 = (\rho C/n) T_0 F_w$ (where n is the whisker resistivity, C is its heat capacity, ρ is the density and T_0 is the vaporization temperature) and the plasma axial expansion velocity. Parker⁹ indicates the range of T_0 to be from 10 to 100 nsec for materials such as used in this experiment. The typical plasma axial expansion velocity is 2-4 cm/ μ sec, associated with a temperature of few eV. Its density is 10^{17} to 10^{19} cm $^{-3}$ for high current diodes and $\sim 10^{15}$ cm $^{-3}$ for low current diodes. Plasma can also be formed at the anode by virtue of the electron beam depositing its energy in the anode and heating it.¹⁹

Another mechanism for plasma production, which has not been investigated in connection with single-pulse diode studies, is that of plasma formation at both electrodes due to a current flow after the diode impedance has collapsed to very low values. This plasma formation mechanism is that of a low voltage vacuum arc,¹⁸ which is driven by the current remaining in the storage system, and because of the nature of inductively driven systems is more pronounced than in pulse-line driven systems. It is convenient to consider separately the two types of plasma: the whisker plasma, generated as a result of very high electric fields, and the arc plasma that arises from the post-pulse current flow and provides a long-time short circuit across the diode.

The results obtained here indicate that indeed a whisker plasma is formed and closes the gap at an average speed of $3-5 \times 10^6$ cm/sec, after which the diode current is being carried primarily by arc plasma in the diode. This current is supported by the energy remaining in the storage system. The arc plasma is observed by the photomultiplier to disappear rapidly (~ 10 μ sec) as seen in Fig. 9, when the current flow is stopped by opening fuse wire $F_{D1,2}$, (Fig. 1).

Two mechanisms by which the plasma density in the diode can decrease after the diode current is stopped are plasma radial expansion (perpendicular

to the diode axis) and recombination. The effect of plasma expansion can be estimated assuming that the plasma ceases to affect the diode impedance when

$$n_p < n_{CL} = J_{CL}/e\beta c \quad , \quad (1)$$

where n_p is the plasma density, J_{CL} is the Child-Langmuir electron current density, n_{CL} is electron density associated with J_{CL} , c the velocity of light, e the charge on an electron, and βc is the beam velocity ($\beta^2 = 1 - (1+eV_D/E_0)^{-2}$ where E_0 is the electron rest energy). Note that data from the Gamble II generator supports the criterion (1). A description of the Gamble II generator operated at much higher diode current density, can be found in Ref. 21. We further assume that the total number of plasma particles is constant (i.e., recombination is neglected after plasma production has ceased) and that n_p is spatially uniform and decreases in time as

$$n_p(t) = n_0 \frac{r_0^2}{r(t)^2} \quad , \quad (2)$$

where n_0 is the initial plasma density and $r(t) = (r_0 + v_r t)$ is the plasma radius at time t resulting from radial expansion at speed v_r . Equating n_{CL} from Eq. (1) with the plasma density from Eq. (2) gives the time τ_{CL} , when plasma no longer affects the diode impedance:

$$\tau_{CL} = \frac{r_0}{v_r} \left[\left(\frac{n_0}{n_{CL}} \right)^{1/2} - 1 \right] \quad . \quad (3)$$

For $V_D = 150$ kV, $\beta = 0.63$ and with a diode separation of 1.5 cm the (non-relativistic) Child-Langmuir Law gives $J_{CL} = 60$ A/cm². From Eq. 1, $n_{CL} \approx 2 \times 10^{10}$ cm⁻³. Assuming $n_0 \approx 10^{16}$ cm⁻³, $r_0 = 1.5$ cm (the diode radius) and using $v_r = 2.3$ cm/μs, which is the average radial speed obtained from streak photography, then by Eq. 3 τ_{CL} is ≈ 500 μsec. (v_r is measured midway between the cathode and anode. It is, within measuring accuracy, equal to axial electrode gap closing velocity.)

An estimate of the recombination (three body and radiative) time²², τ_R , for various carbon and iron plasmas, assuming the density is constant in time, gives $\tau_R \approx 100$ μsec. This estimate is more sensitive to the density ($\sim n_p$) than the estimate of τ_{CL} . Nevertheless, the two time scales

are comparable, $\tau_R \approx \tau_{CL}$ and are close to the experimentally observed time for recovery to type 1 operation of Fig. 12.

To elucidate this point further, the system was also operated in the single pulse mode at various base pressures. Again in analogy to Fig. 4 and 11, the diode current and voltage, collector current, and diode impedance are plotted for base pressures of 10^{-5} , 10^{-3} , and 10^{-2} Torr in Fig. 13. The rapid diode current increase and lower diode voltage characteristics of type 2 discharges are qualitatively reproduced at pressures $> 10^{-3}$ Torr. It therefore appears reasonable that neutrals present in the anode-cathode gap have some effect on the diode recovery. The diode impedance at maximum voltage and maximum collector current is plotted as a function of base pressure in Fig. 14. Note that no data is produced when the base pressure is $\gtrsim 2 \times 10^{-3}$ Torr. The effects of any plasma remaining in the diode have not been investigated.

VI. CONCLUSION

We have demonstrated that moderate energy, ~ 150 keV, electron beam of ~ 1 kA current at densities of ~ 50 A/cm² and pulse duration of ~ 500 nsec can be produced from a low voltage, $\lesssim 10$ kV, inductive storage system. Furthermore, the system can be doubly pulsed with a variable interpulse separation time of 10-500 μ sec.

The diode can recover in times $\gtrsim 100$ -200 μ sec depending on the cathode material. The recovery is not total, even with a 500 μ sec inter-pulse separation time, in that the detailed time histories of the beam current and voltages are not identical for the two pulses. This is most likely due to the presence in the diode of a low level of plasma and neutrals associated with the first pulse (although the second pulse circuitry may also contribute to some of the differences). The choice of parameters in the work described here is reasonable for scaling these results to diodes operating in the megavolt and tens of kiloamperes regime.

ACKNOWLEDGEMENTS

The authors wish to acknowledge the expert technical assistance of Mr. H. Hall, and useful discussions with Drs. R. A. Meger and F. L. Sandel. We also are grateful to Dr. W. Lupton for a critical reading of the manuscript.

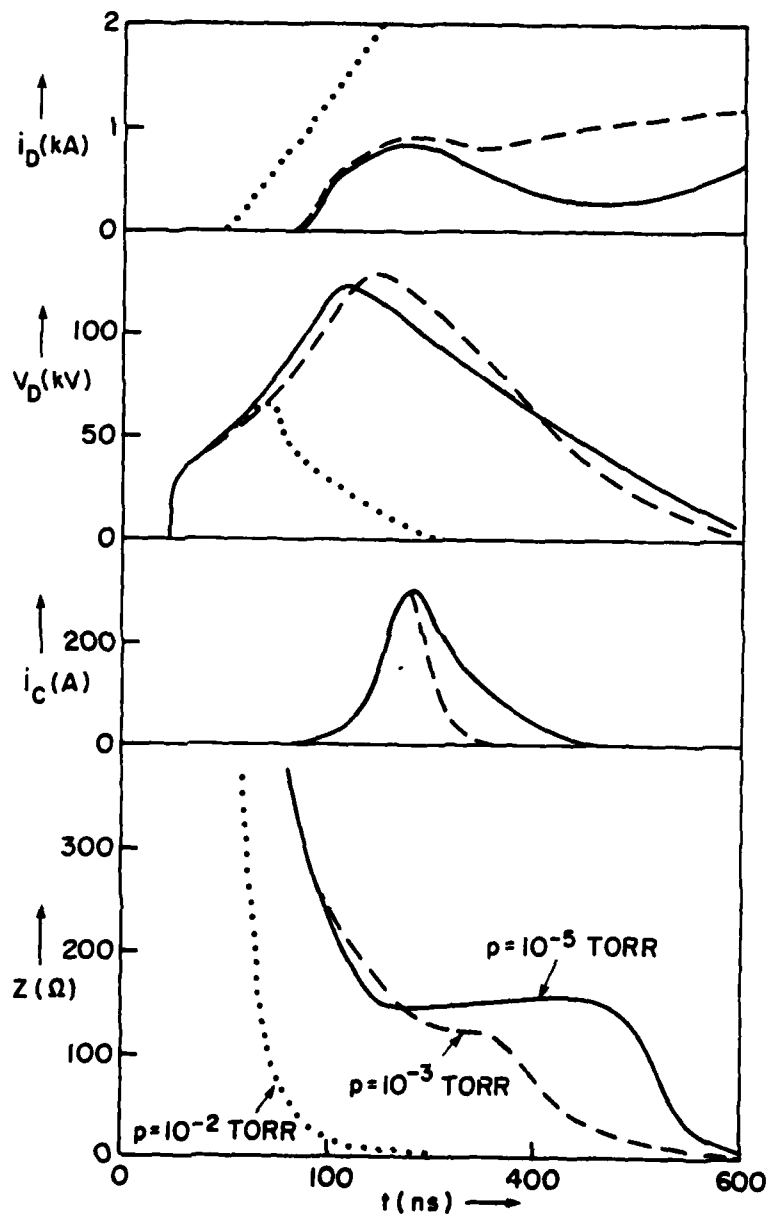


Fig. 13. Diode current, i_D and voltage, V_D , collector current, and diode impedance, Z (V_D/i_D), as a function of time for base pressure of 10^{-2} , 10^{-3} , and 10^{-5} Torr.

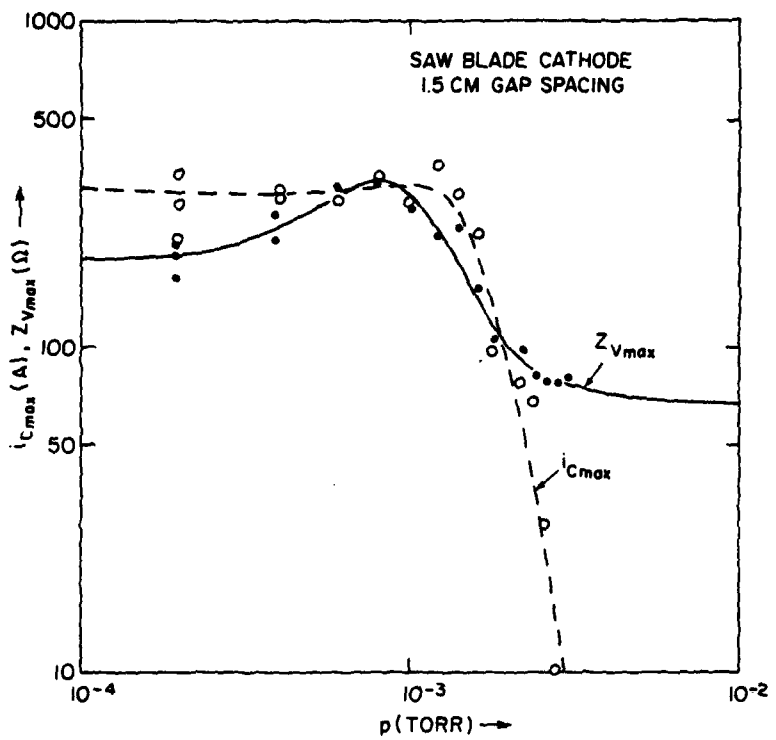


Fig. 14. Diode impedance at maximum voltage and maximum collector current as a function of base pressure.

REFERENCES

1. R. F. Farnsler, D. Conte, and I. M. Vitkovitsky, IEEE Trans. on Plasma Sci. PS-8, 176 (1980).
2. J. E. Eninger, Proc. of the Third IEEE International Pulsed Power Conference, Albuquerque, NM (1981) paper 27.1, to be published.
3. Yu. A. Kotov, B. M. Kovalchuk, N. G. Kolganov, G. A. Mesyats, V. S. Sedoi, A. L. Ipatov, Sov. Tech. Phys. Lett. 3(9), 359 (1977).
4. B. M. Kovalchuk, Yu. A. Kotov, G. A. Mesyats, Sov. Phys. Tech. Phys. 19(1), 136 (1974).
5. J. Salge, U. Braunsberger, U. Schwarz, First International Conference on Energy Storage, Compression and Switching, Torino, Italy (Plenum Press, NY, (1979).
6. I. M. Vitkovitsky, D. Conte, R. D. Ford, W. H. Lupton, NRL Memorandum Report 4168, Naval Research Laboratory (1980).
7. R. D. Ford, I. M. Vitkovitsky, IEEE Trans. on Electron Devices ED-26, 1527 (1979).
8. M. T. Butram, Proceedings of the Second IEEE International Pulsed Power Conference, Lubbock, Texas, IEEE Cat. No. 79CH1505-7 (1979).
9. R. K. Parker, R. E. Anderson, C. V. Duncan, J. App. Phys. 45, 2463 (1974).
10. L. V. Dubovoi, I. M. Roife, E. F. Seredenko, B. A. Stekolnikov, Efremov Institute Report No. OT-5, Leningrad, USSR, (1974).
11. M. Friedman, M. Ury, Rev. Sci. Instr. 41, 1334 (1970).
12. A. S. Gilmour, Jr., R. F. Hope III, R. N. Miller, Conf. Record of the IEEE 14th Pulse Power Modulator Symposium, IEEE Cat # 80 CH 573-5 ED (1980), pp. 80-84. also pp. 247-253.
13. I. M. Vitkovitsky, V. E. Scherrer, J. App. Phys. 52, 3012, (1981).
14. V. Braunsberger, J. Salge, U. Schwarz, Proceedings of the Eighth Symposium on Fusion Technology, Noordwijkerhout, the Netherlands (1974).
15. J. N. DiMarco, L. C. Burkhardt, J. Appl. Phys. 41, 3894 (1970).
16. C. Maisonnier, J. G. Linhart, and C. Gourlan, Rev. Sci. Instr. 37, 1380 (1966).

17. R. D. Ford and M. P. Young, *Proceedings of the Eight Symposium on Fusion Technology*, Noordwijkerout, the Netherlands (1974).
18. T. H. Lee "Physics and Engineering of High Power Switching Devices," Chapters 5 and 6, MIT Press, Cambridge, MA, (1975).
19. A. E. Blaugrund, G. Cooperstein and S. A. Goldstein, *Physics of Fluids*, 20, 1185 (1977).
20. E. J. Henley, D. Richman, *Analytical Chem.* 28, 1580 (1956).
21. L. S. Levine, I. M. Vitkovitsky, *IEEE Tran. Nuc. Sci.* NS-18, No. 4, 255 (1971).
22. R. C. Elton, "Methods of Experimental Physics," Vol. 9A, H. R. Griem and R. H. Lovberg, eds., (Academic Press, 1970), Ch. 4.

DISTRIBUTION LIST

Air Force Aerospace Propulsion Lab
Wright-Patterson Air Force Base
Dayton, OH 45433

Attn: C. Oberly 1 copy

AF Office of Scientific Research
Bolling Air Force Base
Building 410
Washington, DC 20332

Attn: A. Hyder 1 copy

Central Intelligence Agency
P. O. Box 1925
Washington, DC 20013

Attn: C. Miller/OSI 1 copy

AF Wright Aeronautical Laboratory
AFSC
Wright Patterson Air Force Base
Dayton, OH 45433

Attn: P. Bletzinger 1 copy

Air Force Weapons Laboratory
Kirtland Air Force Base
New Mexico 87117

Attn: W. Baker/DYP 1 copy
A. H. Guenther/AFSC 1 copy
R. Reinovsky/DYP 1 copy

Atomic Weapons Research Establishment
Building H36
Aldermaston, Reading RG 7 4PR
United Kingdom

Attn: J. Martin 1 copy

Ballistic Missile Defense Advanced
Technology Center
P. O. Box 1500
Huntsville, AL 35807

Attn: L. Havard (BMDSATC-1) 1 copy

B-K Dynamics Inc.
15825 Shady Grove Road
Rockville, MD 20850

Attn: I. Kuhn 1 copy

Defense Advanced Research Projects
1400 Wilson Blvd
Arlington, VA 22209

Attn: J. Bayless 1 copy

Defense Technical Info Center
Cameron Station
5010 Duke Street
Alexandria, VA 22314 12 copies

Harry Diamond Laboratories
2800 Powder Mill Road
Adelphi, MD 20783

Attn: A. Stewart 1 copy

Jaycor, Inc.
205 S. Whiting St.
Alexandria, VA 22304

Attn: J. Gillory 1 copy
R. Hubbard 1 copy
D. Tidman 1 copy

Naval Air System Command
Washington, DC 20361

Attn: R. Wasneski/AIR-350F 1 copy

Director
Defense Nuclear Agency
Washington, DC 20305

Attn: Maj R. L. Gullickson 1 copy
Capt H. Soo 1 copy

Maxwell Laboratories
9244 Balboa Avenue
San Diego, CA 92123

Attn: J. Pearlman 1 copy

Mission Research Corp
735 State Street
Santa Barbara , CA 93102

Attn: V. VanLint 1 copy

Naval Research Laboratory
Attn: Name/Code
Washington, DC 20375
Addressee:

Code 2627 - TIC-Distribution 25 copies
Code 4700 - Superintendent 26 copies
Code 4770 - I. Vitkovitsky 25 copies
Code 4763 - R. Greig 1 copy
Code 4770 - V. Scherrer 1 copy
Code 4760 - B. Robson 1 copy
Code 6840 - R. Parker 1 copy

On-Site Contractors:

Code 4770 - R. Fernsler 1 copy
4770 R. Commissio 10 copy
4770 S. Goldstein 1 copy

Naval Surface Weapons Center
Dahlgren, VA 22448

Attn: M. F. Rose/F-04 1 copy
L. Lussen/F-12 1 copy

Naval Surface Weapons Center
White Oak Laboratory
Silver Spring, MD 20910

Attn: R. Biegalski 1 copy
R. Fiorito 1 copy
C. Huddleston 1 copy
L. Miles 1 copy
E. Nolting 1 copy
G. J. Peters 1 copy

Office of Naval Research
800 N. Quincy Street
Arlington, VA 22217

Attn: W. J. Condell/421 1 copy
M. A. Howard/210 1 copy

Research and Development Associates
1401 Wilson Avenue
Arlington, VA 22209

Attn: D. Conte 1 copy

Pulse Science Inc.
Suite 610
1615 Broadway Avenue
Oakland, CA 94612

Attn: I. Smith 1 copy

Science Applications, Inc.
1200 Prospect Street
LaJolla, CA 92037

Attn: M. P. Fricke 1 copy

Science Applications, Inc.
5 Palo Alto Square, Suite 200
Palo Alto, CA 94304

Attn: J. Siambis 1 copy

Science Applications, Inc.
1651 Old Meadow Road
McLean, VA 22101

Attn: W. Chadsey 1 copy

Texas Tech University
Dept. of Electrical Engineering
Lubbock, TX 79409

Attn: M. Kristiansen 1 copy
E. E. Kunhart 1 copy

Physics International, Inc.
2700 Merced Street
San Leandro, CA 94577

Attn: A. Toepfer 1 copy
J. Benford 1 copy

McDonnell Douglas Research Laboratories
Dept. 223, Bldg. 33, Level 45
Box 516
St. Louis, MO 63166

Attn: M. Greenspan 1 copy

Cornell University
Ithaca, NY 14853

Attn: D. Hammer
H. Fleishman

1 copy
1 copy

Avco Everett Research Laboratory
2385 Revere Beach Pkwy
Everett, MA 02149

Attn: R. Patrick
1 copy

Sandia National Laboratories
Albuquerque, NM 87185

Attn: B. Miller/4241
B. Epstein/4241
J. Olsen/4244
P. VanDevender/4252

1 copy
1 copy
1 copy
1 copy

University of California
Physics Department
Irvine, CA 92717

Attn: G. Benford
1 copy

U.S. Army Research Office
P. O. Box 12211
Research Triangle Park, NC 27709

Attn: B. D. Guenther
1 copy

University of South Carolina
College of Engineering
Columbia, SC 29208

Attn: J. E. Thompson
1 copy

Institut Fur Hochspannungstechnik
Technische Universitat Brunschweig
Pockelsstrasse 4 Postfach 3329
3300 Braunschweig, West Germany

Attn: B. Fell
U. Braunsberger
J. Salge

10 copies
1 copy
1 copy

Lawrence Livermore National Laboratories
University of California
Livermore, CA 94550

Attn: R. J. Briggs
1 copy

END

DATE

FILMED

3-82

DTIC